Improving situational awareness for flash flood forecasting in a small urban catchment by integrating meteorological analysis into a geospatial framework

Lesley-Ann Dupigny-Giroux[b], John Goff[a], John Kilbride[b], Jeffrey D. Marshall, Sarah Leidinger[b], Phoebe Fooks[b], Megan Moir[d]

Corresponding author
John Goff
[a]NOAA/National Weather Service Forecast Office/ Burlington VT
1200 Airport Drive
South Burlington, VT 05403
USA
John.Goff@noaa.gov

[b]University of Vermont
Department of Geography
94 University Place
Burlington, VT 05405-0114
USA

[c]University of Vermont
Bailey/Howe Library, Research Collections
538 Main Street
Burlington, VT 05405
USA

[d]Burlington Public Works Department
Water Resources Division
234 Penny Lane
Burlington, VT 05402

1.0 Introduction

Urban flooding is among the more challenging meteorological events from a predictive standpoint. As with flash flooding in rural watersheds, the interrelated factors of land use, topography, antecedent precipitation, and precipitation rate all must be considered when assessing the threat posed by the hazard. In addition, familiarization with favorable synoptic patterns and atmospheric thermodynamic properties is critical in determining the potential for flooding (Maddox et al. 1979). In a recent study, Jessup and Colucci (2012) performed extensive analysis of 187 flash flood events in the Northeastern United States and concluded that some of the most likely flood-producing factors were backward propagating (opposite direction to most storms of similar type) and merging storms. These characteristics were present during the devastating Montgomery, Vermont flash flood event of July 14-15, 1997, described in detail in Dupigny-Giroux et al. (2006).

Average basin rainfall rates and the duration of intense rainfall are arguably the most important meteorological causes of flash flooding. Such drivers were the backbone of the Areal Mean Basin Estimated Rainfall Program (AMBER) developed by Robert Davis in the 1980s and 1990s at the National Weather Service forecast office in Pittsburgh, Pennsylvania (Davis & Jendrowski 1996). When high intensity rainfall persists over a watershed for a longer period of time, storm runoff increases significantly as local soils become saturated (Davis 2003). These interrelated phenomena have been well documented and provide the underlying foundation for the National Weather Service's Flash Flood Monitoring and Predication (FFMP) software (Smith et al. 2000). However, the accuracy of local radar data poses challenges in assessing rainfall rate and intensity. Proper calibration of radar hardware and application of the correct reflectivity-rainfall rate relationships (Z-R) remain critically important in generating accurate precipitation estimates (Einfalt et al. 2004). This can be particularly challenging in areas of radar beam blockage or in locations where rainfall gauge density is low. In addition, Smith et al. (2007) found that as the temporal and spatial scales of a basin decrease, the error in radar-estimated rainfall also increases. Berne et al. (2004) addressed this issue by quantifying the temporal and spatial resolutions necessary for assessing rainfall measurements in the urban environment, finding that a time step of 10 minutes with a spatial resolution of 6000 ha was sufficient under most circumstances. In a similar study, Jensen and Pedersen (2005) found that within a single radar pixel (500 m x 500 m), a relatively high magnitude of variation existed in rainfall totals across an established gauge network, in some cases by a factor of 2. Jensen and Pedersen (2005) concluded that, to best monitor flash flooding or quickly responding urban basins, a radar unit with a 100 m x 100 m resolution and a high density gauge network were necessary. Although the recent installation of dual-polarization software on National Weather Service WSR-88D radars has been shown to improve accuracy in precipitation estimates (Vasiloff 2012), much research is still needed to quantify the complex and interrelated factors governing the threat and severity of the urban flash flood.

In addition to urban watershed modelling, Geographic Information Science (GIS) is commonly used for hydrologic flood analysis due to the flexibility with which datasets can be manipulated and analyzed (Tehrany et al. 2014). The hydrologic response time to very heavy precipitation has been observed to produce flash flooding in several hours (Shih et al. 2014). As such, the spatial queries of precipitation, elevation and hydrologic data can assist government agencies in producing flood assessments and developing warning systems (Diaz-Nieto et al. 2011; Kulkarni et al. 2014; Moawad 2013). GIS-based online flood prediction systems have been successful in alerting regions about potential urban flooding (Bedient et al. 2003; Shih et al. 2014). Other methodologies have utilized the GIS environment as the interface where data are

compiled and combined with hydrologic models (Shahapure et al. 2011; Viavattene & Ellis 2013). Hydrologic models can represent surface and sub-surface flows to identify the infrastructure-related problems that cause flooding (Jahanbazi & Egger 2014; Pathirana et al. 2011). However, the expense and expertise required may make a full hydrologic model cost-prohibitive.

Of particular importance in the observation and forecasting of urban flood events is the spatial density of the existing rain gauge network. Rain gauges provide point measurements of rainfall over a small area, which can then be interpolated to estimate the rainfall over a larger region (Blumenfeld & Skaggs 2011; Huang et al. 2014). While more accurate interpolation results can be derived from well-distributed networks, they must be sufficiently dense to reduce interpolation error (Blumenfeld & Skaggs 2011; Chintalapudi et al. 2012; Yoo et al. 2013). In a study of the Minneapolis, Minnesota metropolitan area Blumenfeld and Skaggs (2011) noted that a gauge density of 9 gauges per 100 km^2 was sufficient to capture the variability in extreme precipitation values. However, the interpolation of a similarly spaced rain gauge network may not accurately replicate the spatial variability of rainfall needed for hydrologic or flooding estimation in small urban environments (Collier 1986). Regions which either lack radar data or which are prone to radar blockage may be forced to rely on these low density rain gauge networks to produce the hydrologic data needed in flood assessments and GIS-based hydrologic models.

Some studies, for example, have found that rain gauge measurements can show significant variability in basins smaller than 2 km^2 (Jensen & Pedersen 2005; Peleg et al. 2013). Jensen and Pedersen (2005) noted that rainfall measurements from a grid of 9 rain gauges arranged within a 0.25 km^2 area could still vary by a factor of 2. Ciach and Krajewski (1999) determined that dense gauge networks were necessary on a sub-radar pixel level in order to resolve issues associated with the radar-rain gauge relationship in the point-area estimation of rainfall. The high spatial density of a 15-rain gauge array set up at an Iowa airport to study the sub-radar pixel variability in rainfall, allowed the researchers to determine the amount of error introduced by gauge measurements and resolve issues associated with capturing the spatial variability of rainfall in a small area (Krajewski et al. 1998). However, the establishment and maintenance of a high density rain gauge network is typically cost-prohibitive and limited to select locations or study sites. Thus, many towns and smaller cities are forced to rely on low density networks which may not capture the inherent spatial variability in intense, short-duration heavy rainfall bursts. In these instances, radar precipitation estimates may provide the best assessment of the potential for urban flooding.

Radar rainfall estimates allow for the higher temporal resolution needed in urban hydrology and flood prediction (Berne et al. 2004; Einfalt et al. 2004; Smith et al. 2007) with NEXRAD data being a more cost effective method of obtaining rainfall estimates for flood analysis in many cases. While radar data are a suitable alternative to rain gauge networks for hydrologic modeling and flood prediction in large catchments (on the order of 10,000 km^2), similar utilizations of radar data in small urban catchments (<20 km^2) have remained relatively unexplored (Knebl et al. 2005; Smith et al. 2013). Case studies which evaluated flooding in urban environments have found that NEXRAD data can be used to accurately represent the observed flow in sewers and streams (Bedient et al. 2003; Brauer et al. 2011; Knebl et al. 2005). Creutin et al. (2009) noted that smaller watersheds or sub-catchments will respond faster to extreme precipitation events than larger basins. Radar's high temporal resolution is therefore important to real-time flood prediction in communities with small urban basins characterized by fast hydrologic response times.

One of the unique characteristics of urban flooding is the significant role played by impervious surfaces and stormwater systems in runoff efficiency. Historically, many natural

watercourses have been buried by years of development. Today, these natural water courses are often invisible and poorly mapped, although they still act as foci for near and subsurface runoff. Original sewer and storm water systems constructed during the late 1800s and early 1900s often follow these now buried watersheds. As these human systems have become antiquated by over a century of development, they now serve as conduits for flooding during high intensity rainfall events and are problematic for municipal planners. This important challenge has been addressed by modelling urban watersheds and their response under these types of precipitation events. Mark et al. (1998) used the MOUSE modelling system to simulate flooding in Dhaka City, India, thereby demonstrating how sewer systems could be optimized to prevent urban flooding and the harmful transport of pollutants. Other efforts included the modelling of Tropical Storm Allison's flooding in Houston, TX (Bedient et al. 2007), and the development of a hydrologic model for the Pocono Creek in eastern Pennsylvania through the use of radar data and a soil water assessment tool (Kalin and Hantush 2006).

A common thread through these and similar studies is their focus on individual events or storm drainage networks, thus, highlighting the unique nature of a given urban basin's susceptibility to flooding. Examples of such basin-specific urban flooding have occurred in the city of Burlington, VT where six discreet events were observed in the one-year period between 4 July, 2012 and 4 July, 2013. Surprisingly, much of the observed flooding during these events occurred in the same locations, in particular along a long-buried, natural ravine that runs through the heart of the city.

As a result of the recent flooding events, the Burlington municipal Public Works Department began a wholesale update of their hydraulic and hydrologic models for the main sewer collection system in 2014, a portion of which runs the length of the old ravine (Burlington Public Works 2014). These hydrologic and hydraulic models are providing the Department with a better representation of the combined sewer/storm water collection system and runoff generating mechanisms via heavy rainfall simulations. In addition to this work, construction projects to improve poor drainage issues at the juncture of Main St. and South Winooski Avenue were completed in late 2013 and a proposal is currently underway to help alleviate similar flooding problems in the vicinity of Pine Street (Fig. 1). These combined efforts will ultimately help the Department to evaluate the impacts of future flood events, and explore various alternatives for mitigating such issues.

This paper seeks to advance our understanding of the hydrological challenges which may be unique to the City of Burlington, Vermont while providing a methodological framework to explore urban flooding in similar contexts. It quantifies urban flooding in the vicinity of the old ravine via meteorological and geospatial analyses within the historical context. Content analysis of the National Weather Service (NWS) Storm Data publication and the Burlington Free Press archives were used to determine the prevalence of and pre-disposition towards flooding over the last 150-200 years. GIS technology was used to investigate the spatial distribution of selected flooding episodes. Short duration rainfall rates, antecedent precipitation and intensity-frequency-duration data were used to highlight the importance of using high temporal frequency data in urban catchments, a fact which was underscored by case studies of two recent flood events. Finally, the paper highlights the invaluable insights gained from the use of sub-hourly rainfall intensity estimates from the dual-polarized KCXX WSR-88D radar rather than the coarser resolution legacy data historically used over this small urban catchment.

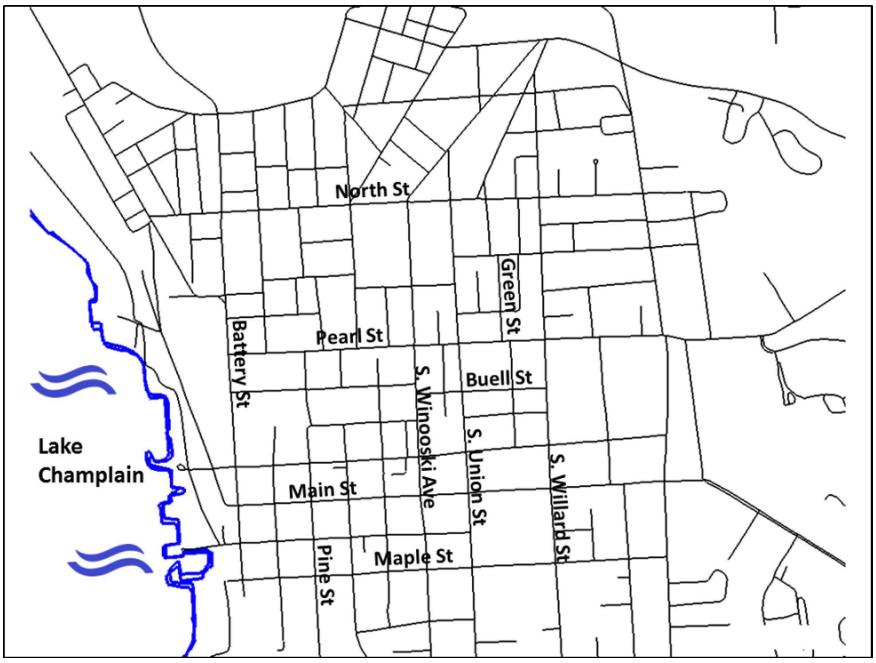

Figure 1 Sketch map of the City of Burlington, Vermont showing the major streets referred to in the text.

2.0 Materials and methods

The urban center of Burlington, Vermont lies near 44.47°N, -73.21°W, on the eastern shores of Lake Champlain. From the relatively flat lakeshore at approximately 30.48 m (100 feet) MSL, the topography abruptly increases in elevation via a series of terraces to 45.72-91.44 m (150-300 feet) to the east and northeast, terminating in an arcing escarpment which separates the City from the larger Winooski River basin. To the south, the terrain is flat to gently rolling with several small watersheds draining directly into the Lake. Although identifiable streams and watercourses are difficult to discern in this heavily urbanized city center, general drainage is in a west to southwesterly direction towards the Lake. The study area for this paper is the small watershed which encompasses the old ravine drainage, with an area of only 3.44 square kilometers (1.33 sq. mi.) (Fig. 2).

The story of Burlington's lost ravine is a long and colorful one, with maps as early as the 1850s showing the distinct topographical feature extending northeast to southwest through the main urban corridor to its mouth on the shore of Lake Champlain (Fig. 3). The ravine was quite deep, extending perhaps to a depth of 100 feet in places. Maps from 1869 and 1872, show not only the outline of the ravine, but several small depressions and a large pond along it as well (Figures 3, 4a). This deep topographic feature was traversed by bridges along the two main east-west roads into Burlington (Pearl Street and Main Street) by the 1830s. It served as a primary conduit for the Vermont Central Railroad from 1850 to 1862, after which the track was rerouted to avoid the steep grade required to enter the ravine at its northern terminus (Fig. 4b). Perhaps most problematic were the poor drainage and sanitation issues in the vicinity of the small basin after periods of heavy rainfall.

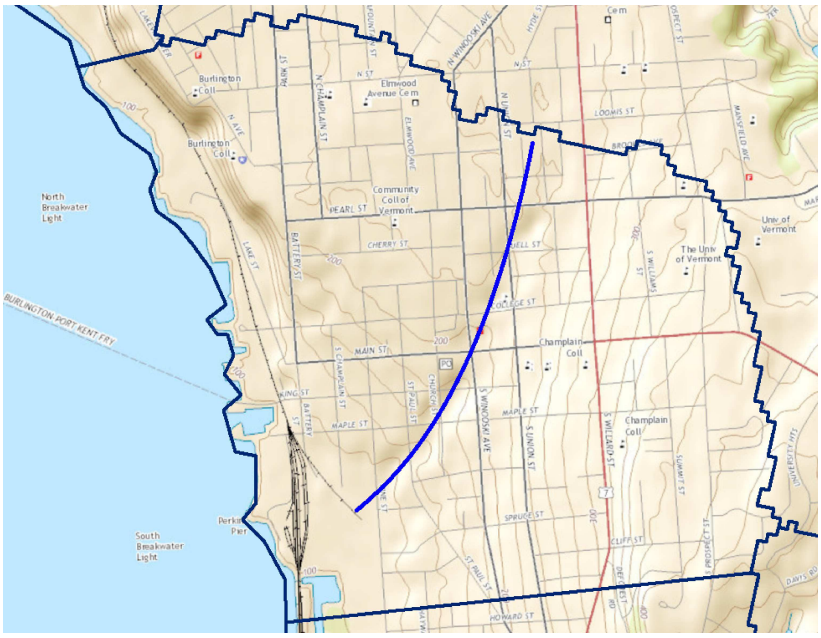

Figure 2 Present-day map of the City of Burlington, Vermont showing the location of the former ravine (blue line running north-northeast to south-southwest) and the outline of the 3.44 km^2 (1.33 mi^2) urban catchment used by the National Weather Service Forecast Office Burlington.

As the village of Burlington grew rapidly in the 1860s, the need for urban infrastructure was one of the factors that led to its achieving a city charter from the Vermont General Assembly in 1865. The new city soon built a public water system, and turned its attention to public sanitation. The building of a sewer system proceeded at a much slower pace, and was not substantially completed for several decades. At its center, Burlington's main sewer followed the course of the ravine, and most of the smaller lines were connected to it. These sewers handled both household/commercial waste as well as storm and snowmelt runoff. Periods of heavy rainfall were marked by poor drainage and sanitation concerns in this small urbanizing catchment. Although continued improvements in the system were able to address the most troublesome sanitation issues by the turn of the 20th century, flooding episodes were still noted during periods of excessive rainfall over the next 100 years. By the early 2000s, portions of the sewer system had become antiquated as choke points arose between older pipes and the more contemporary storm water infrastructure. In addition, the area along the original ravine had become heavily urbanized, increasing the flashiness of runoff during periods of intense rainfall.

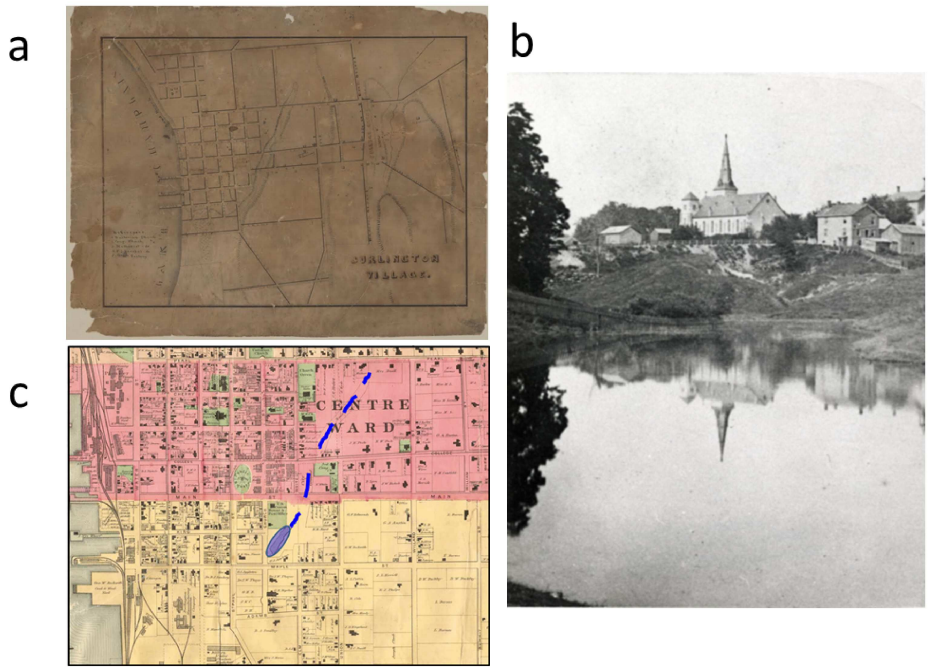

Figure 3 Historic images of Burlington Village, Vermont: a) Map of the village (ca. 1830s) showing the ravine running north-northeast to south-southwest (creator unknown), Special Collections, University of Vermont Libraries; b) Small pond (indicated by blue shaded oval on part c), looking northeast towards the Third Congregational Church at the corner of College Street and South Winooski Avenue (ca. 1870); c) 1869 Beers map highlighting the location of the ravine (dashed blue lines) and pond bounded by Maple and Church Streets.

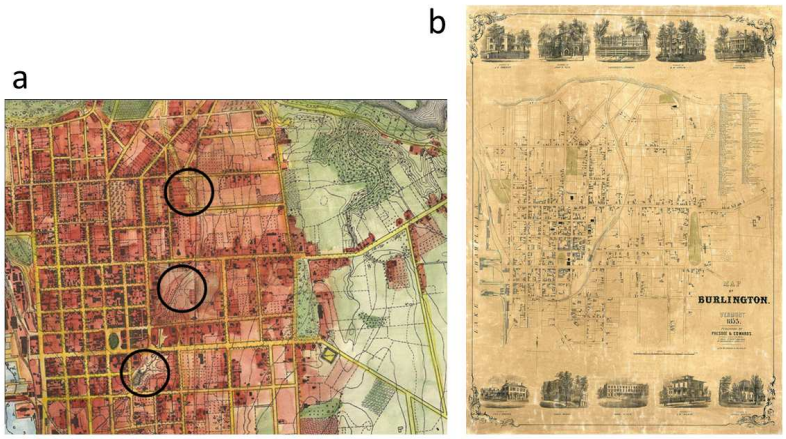

Figure 4 Historical maps of Burlington, Vermont showing a) the larger catchment of the ravine with small depressions and the pond (Figure 3c) on the 1872 Coast Survey map; b) Vermont Central Railroad's route along the ravine on the 1853 Presdee and Edwards map.

2.1 Meteorological analyses

To gain a perspective on the historical frequency of urban flooding in the city of Burlington, VT, warm season1 flood events documented from the early 20th century through

[1] For the purposes of this paper the warm season is defined as the months of April through September inclusive.

September 2013 were compiled from the NWS Storm Data publication, and archives of the Burlington Free Press newspaper available at the Fletcher Free Library (Burlington, VT). To improve efficiency in the search technique several steps were incorporated. In step one, all days on which at least 25.4 mm (1 inch) of rainfall was observed at the Burlington International Airport (KBTV) were compiled from 1939-present. The airport lies approximately 4.8 km (3 miles) east of the center of the city center, with first-order data from 1930 to the present. The length and accuracy of these data made the KBTV records the best proxy for heavy rainfall episodes and subsequent flooding events in Burlington, despite the caveat of the inherent variability of convective rainfall. The daily threshold of 1 inch (25.4 mm) for a heavy rainfall event was chosen to coincide with current operational practices and observations at the NWS Forecast Office in Burlington, VT, and was a good approximation of daily precipitation totals with a higher likelihood of producing widespread urban flooding. To further narrow down the dates on which flooding potentially occurred, for each of the 25.4 mm (1 inch) precipitation dates, hourly rainfall rates were examined with the additional criterion of at least 25.4 mm (1 inch) of rainfall falling within a one hour period. For precipitation observations that spanned the top of a particular hour, they needed to equal or exceed the standard American Meteorological Society's definition for heavy rainfall rates of 7.62 mm (0.30 in) hr^{-1} for each hour. Dates which met all of these criteria were categorized as heavy rainfall events for the purposes of the study. Given that hourly data only began in 1948, this further limited the sample pool from which to draw identifiable events. This date selection process yielded 67 discrete heavy rainfall days with reports of flooding from the two sources occurring on 28 days, or approximately 42 percent of the records available.

Given the strong influence of precipitation intensity and basin rainfall rates on urban flooding, box and whisker quartile analysis was performed on all 67 events to determine the relative importance of short term precipitation rates (1 hour or less) during flood and null (non-flood) episodes. These were obtained through the NWS Local Monthly Climatological Data (LCD), available online from the National Oceanic and Atmospheric Administration's National Center for Environmental Information (formerly the National Climatic Data Center (NCDC)), available at http://www.ncdc.noaa.gov. Maximum hourly rates were obtained for each event, with those occurring after 1998 reported from the NWS Automated Surface Observing System (ASOS) platform at KBTV. Short duration precipitation rates at 15, 30, 45 and 60 minute time steps were also extracted from NWS Local Climatological Data and evaluated. One limitation in using these shorter time steps was that only the individual dates with the heaviest sub-hourly rates were listed for any given month, reducing the complete number of heavy precipitation event days from 67 to 44, with 17 of those, or approximately 39 percent having reports of discrete flooding. Finally, to gauge the potential importance of soil saturation or wetness to the flood events, antecedent 1 and 2-week precipitation was calculated for all 67 events (both flood and null).

2.2 Geospatial data

Two types of geospatial data were acquired and manipulated in the ESRI ArcGIS software platform. Historical imagery was acquired from the University of Vermont's Special Collections at the Bailey-Howe Library, and from the Library of Congress. The historical maps were georectified in the ESRI ArcGIS software program, allowing the original topographic features of the urban center to be digitized into high resolution GIS map layers for overlaying with contemporary flood episodes. The ravine was digitized from an anonymous 1850's map of Burlington's sewer system (Library of Congress 2016) (Fig. 5)**.** Using flooding reports extracted from the archives of the Burlington Free Press newspaper, a map layer of flood locations was

also created and graduated symbology used to highlight repeated events (Fig. 6). Due to the varying levels of detail for the exact locations of the flooding in these historical reports, markers were either placed a) at the center of a road intersection, if two roads were named or b) the center of a building if flooding was reported at a given building. In addition, these textual locations were supplemented through the use of photographs and video news reports of flooding. Finally, non-specific flood report locations (e.g. "Flooding on South Winooski Ave.") were omitted from this map layer.

The second type of geospatial data were high resolution layers acquired from statewide and municipal sources. The 0.5 m orthophotos, the 3.2 m Digital Elevation Model (DEM), and the corresponding slope and hillshade data layers (Figures 5, 6) of Chittenden County, Vermont were accessed from the Vermont Center for Geographic Information. The 2 ft contour lines for the City of Burlington were produced by the UVM Spatial Analysis Lab. The Burlington Department of Public Works provided ArcGIS layers of the locations of storm water sewer lines, storm water inlets, catch-basins, and other relevant features to Burlington's storm water system (not shown). Together, these data allowed conclusions to be drawn about the role of orography, presently buried topographic features and drainage in contributing to the preferred flooding locations in the urban center of Burlington, VT.

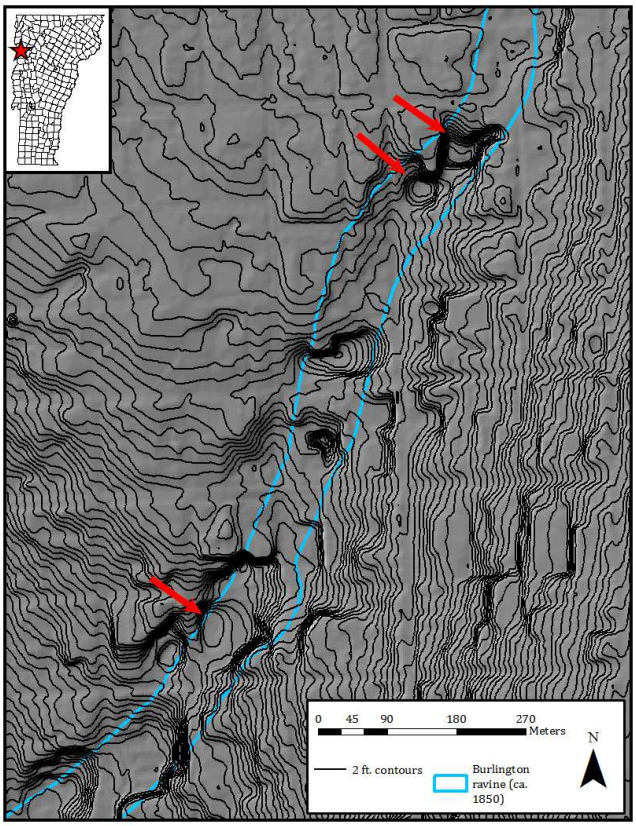

Figure 5 Hillshade layer (gray) created from 2 foot contour lines (superimposed in black), with an overlay of the ravine outline (blue) as digitized from ca. 1850s Library of Congress "[p]lan of the city of Burlington shewing [i.e. showing] water & sewer service" (available at <https://www.loc.gov/item/2011589282/>. Depressions along the ravine are highlighted in red.

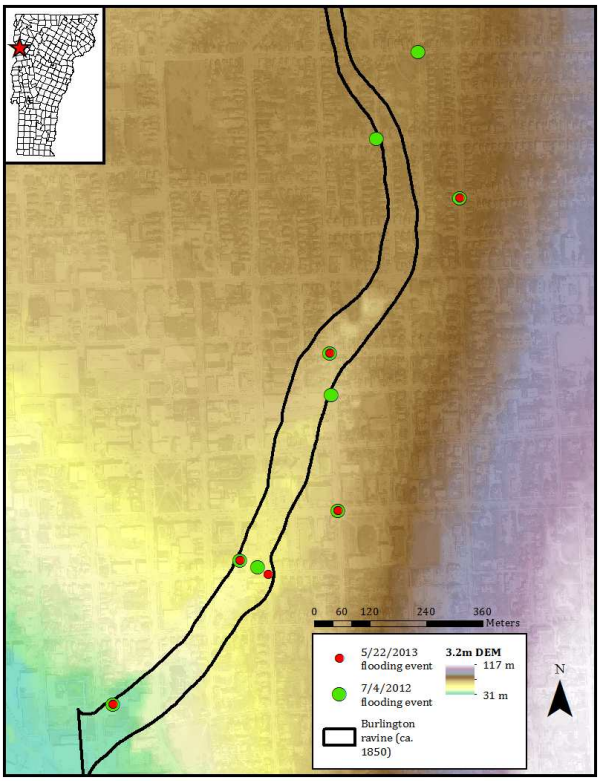

Figure 6 High resolution (3.2m) Digital Elevation Model (DEM) and 1850 digitization of the ravine draped on 0.5m orthorectified photographs. The locations of flooding reports in the Burlington, VT catchment are shown on a) 4 July 2012, b) 22 May 2013 (green) and 4 July 2013 (red).

3.0 Results and discussion

3.1 Historical Frequency of Flooding

Of the 67 heavy rainfall days identified between April 1948 and September 2013 at the Burlington International Airport (KBTV), 28 (42 percent) coincided with reports of varying magnitudes of flooding in the City of Burlington (Fig. 7a). Content analysis of the Storm Data and Burlington Free Press articles revealed direct references to flooding along the former ravine as well as generic descriptions (neither coordinates nor streets/intersections given) at other locales around the city. The lack of perfect overlap between heavy rainfall and actual/reported flood events could be due to the inherent variability of convective rainfall distribution over short distances and the temporal scales involved. In addition, the 4.8 km (3 mile) distance between KBTV and the Burlington city center and former ravine, is a critical factor in accounting for large differences in precipitation rates and amounts between the two locations during any given event. The lack of complete correspondence among flooding reports from the various qualitative sources may be a function of the subjectivity with which severe flooding was reported. While not addressed in this study, this subjectivity in the use of qualitative flood records raises the question of how to properly classify an urban flood event. Evidence of this subjectivity included the documentation of “nuisance ponding” or basement flooding in the archival materials, vis-a-vis the costlier, large scale events. This may have led to the omission of minor flood or nuisance events in the historical record, and, therefore, a reduction in the sample pool used.

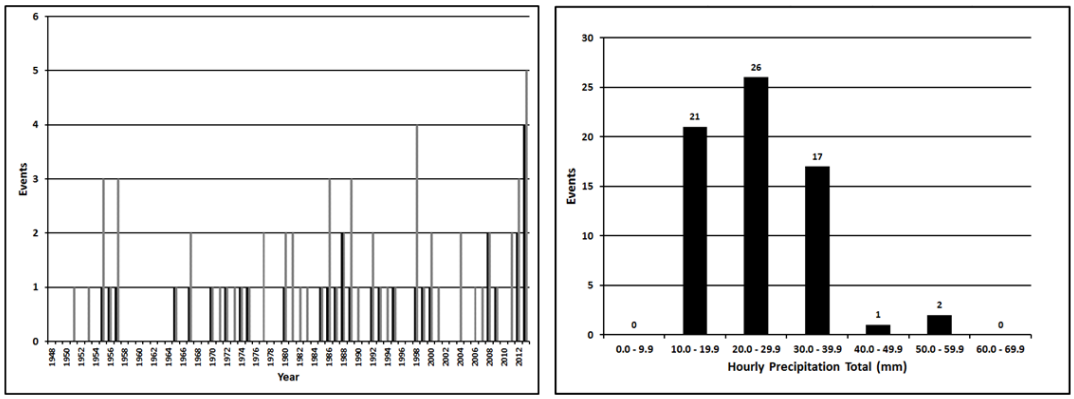

a b

Figure 7 a) Number of events observed during heavy rainfall, null events (black) vs. flood-producing heavy rainfall events (grey); b) METAR-based maximum hourly precipitation rates (mm) observed during heavy rainfall events. All data were for April-September of 1948-2013 at Burlington, VT. (Source: National Center for Environmental Information).

3.2. Short-term precipitation rates

3.2.1 Hourly rates

In general, flash flooding is driven by several interrelated factors, not the least of which is short term precipitation rate and intensity (Doswell III et al. 1996). To gauge the influence of high intensity, short duration precipitation along the ravine and in the city of Burlington proper, a frequency distribution of the hourly rainfall totals for each event was plotted (Fig. 7b). The data show a nearly normal distribution centered around 20-30 mm h^{-1}, with a distinct right hand tail. This is not surprising given that tropical air masses with high precipitable water content (> 50 mm) and excessive hourly rainfall totals (> 50 mmh^{-1}) are relatively uncommon at Burlington's northerly latitude (44.47 N). In fact, only two events in the 65-year study period exhibited hourly rates in excess of 50 mm.

3.2.2 Sub-hourly rates

In the urban environment, the importance of short duration precipitation on the sub-hourly time scale can play an even greater role in the overall flood threat. Thus, sub-hourly precipitation rates from NCDC monthly LCD publications were analyzed for all flood and null events at 15, 30, 45 and 60 minute increments. Data limitations included a start date of 1971, with gaps in the record due to inconsistencies in ASOS hourly values. This limited the analysis to 44 of the 67 total events with 19 of those being flood days. Box and whisker plots revealed that median rates averaged 2-5mm more for flood versus null events, with the largest sub-hourly differences occurring at the 30-minute time step (4.07 mm) (Fig. 8). These differences were statistically similar with F-test analysis indicating nearly equal mean variances of both flood and null datasets at each time step (Fig. 9). Closer investigation of this seemingly innocuous result revealed that the median precipitation values for all flood events (17) were near or slightly above 25 mm at the 30 and 45-minute time step, with several cases having totals approaching 25 mm at

the 15-minute increment. The relative scarcity of hourly rates in excess of 50 mm at KBTV suggests that sub-hourly rates at or above 25 mm are of greater importance in assessing the urban flood threat in the Burlington area. This is reflected in precipitation-intensity-frequency duration plots for the City for both 2 and 5 year return intervals (Fig. 10). Both plots show that, while hourly rates in excess of 25.4 mm (1 inch) are uncommon, intense short-duration precipitation bursts with rates greater than 76.2 mm (3 inches) per hour do occur on these time scales. It is likely that these intense, short-duration events are the most problematic when addressing the causality of urban flood events within the City during the warm season.

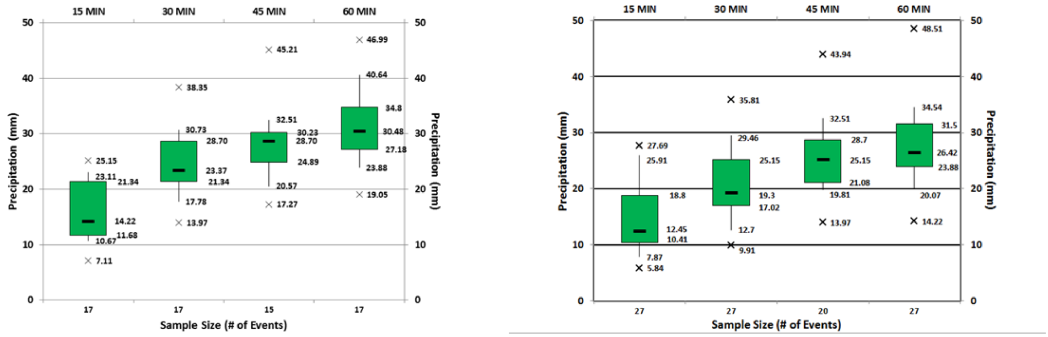

a b

Figure 8 Box and whisker plots for short duration precipitation observed during a) flood-producing, heavy rainfall events and b) heavy rainfall, null events at Burlington, VT for April-September of 1971-2013. As per convention, the boxes represent the 25-75th percentiles, whiskers the 10th and 90th and "x" were extreme values.

SHORT DURATION 15 MIN	NULL	FLOOD
Mean	0.567407	0.647059
Variance	0.058043	0.048122
Observations	27	17
df	26	16
F	1.206162	
P(F<=f) one-tail	0.354624	
F Critical one-tail	2.219593	

SHORT DURATION 30 MIN	NULL	FLOOD
Mean	0.827407	0.971176
Variance	0.071781	0.059574
Observations	27	17
df	26	16
F	1.204922	
P(F<=f) one-tail	0.355452	
F Critical one-tail	2.219593	

SHORT DURATION 45 MIN	NULL	FLOOD
Mean	1.017	1.101333
Variance	0.067222	0.065712
Observations	20	15
df	19	14
F	1.022975	
P(F<=f) one-tail	0.492216	
F Critical one-tail	2.400039	

Figure 9 F-test results highlighting the near equal variances of the short term precipitation rates (in.) observed during both flood-producing heavy rainfall events and null ones, at intervals of 15, 30 and 45 minutes.

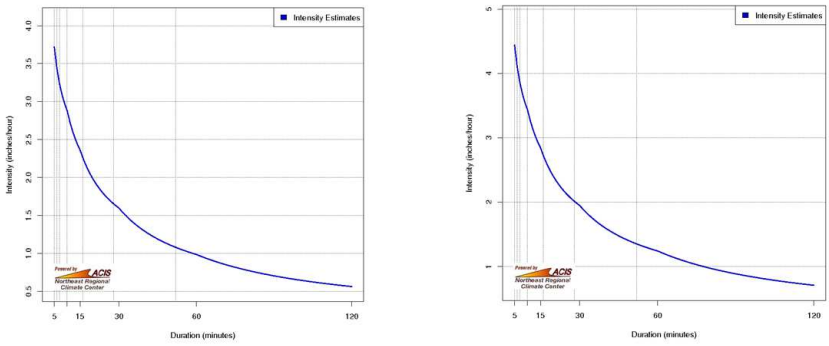

Figure 10 Intensity-duration-frequency (IDF) curves for Burlington, VT for the a) 2 year return interval and b) 5 year interval. (Figure courtesy of the Northeast Regional Climate Center).

3.3 Antecedent precipitation

In addition to the rainfall rate, antecedent precipitation and the limited capacity of near-saturated ground to absorb additional rainfall are important factors in assessing the threat of urban flash flooding. Using the knowledge that many flash floods occurred during periods of

abnormal wetness, especially across the northeastern United States (Jessup and DeGaetano 2007), antecedent 1- and 2-week precipitation data for all flood and null events were analyzed. As expected 1 and 2-week precipitation totals for flood events were greater than null events (Fig. 11). Plots show that 1 week totals averaged 29.02 mm for flood producing events, and 21.33 mm for null events. Similarly, 2 week totals averaged 51.02 mm for flood events and 46.44 mm for null events. While the larger difference (7.69 mm) between the flood producing totals versus the null events was observed at the 1-week time interval, the relative similarity in the actual totals again may be attributable to omissions in the historical record or variability in convective rainfall distribution. It is important to note that the role of antecedent precipitation in Burlington's urban flood history is not insignificant, as indicated by examining the antecedent raw data where the 1-week rainfall prior to several flood episodes, exceeded 50 mm. For example, the significant flooding observed on 17 August, 1955 was preceded by a 1-week rainfall total in excess of 100 mm. However, given the more complex and interconnected factors governing precipitation runoff in the urban environment, influence of antecedent precipitation during any single event may be less than precipitation of similar magnitudes falling in rural or more pervious environments.

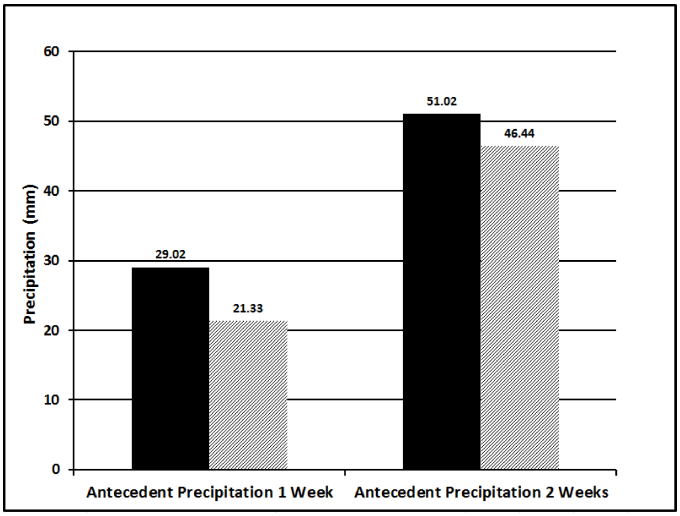

Figure 11 Mean antecedent precipitation (mm) for the 1 and 2 week timeframes for the flood (hatched) versus the null (black) events at Burlington, VT for April-September of 1948-2013.

3.4 Case studies

Two case studies (4 July, 2012 and 22 May, 2013) were selected for widespread flooding of city infrastructure, particularly along the old ravine where clogged storm drains and rapid surface runoff occurred. It should be noted that only legacy KCXX WSR-88D precipitation estimates were available for the 2012 case. The KCXX WSR-88D radar (located in Colchester, VT, approximately 4.8 km northeast of the study area) was upgraded with dual-polarization (DP) technology in late July 2012, allowing for a discrete comparison between both the DP-based and legacy quantitative precipitation estimate (QPE) algorithms for the May 2013 case study. The goal of this comparison was to determine whether the DP QPE algorithms provided an improved observation tool for a small urban watershed. METAR observational data and radar precipitation estimates were used to examine the importance of short duration, high intensity precipitation as a trigger for urban flooding on these two dates. Precipitation Intensity-Duration-Frequency (IDF) data from the Northeast Regional Climate Center (NRCC) provided an independent verification

of intense, short duration precipitation rates as the most important meteorological factor governing urban flood potential in the city.

3.4.1 Case study 1 - 4 July, 2012

From approximately 2315 to 2345 UTC on 4 July, 2012 the City of Burlington experienced a severe thunderstorm event with hail, high winds and heavy precipitation (Fig. 12). At KBTV, observed wind gusts from this system exceeded 25 ms^{-1} (50 kt) (Table 1). More problematic was the intense, short duration rainfall burst which led to rapid urban runoff and resultant flooding in portions of the City. At KBTV, nearly 25 mm of precipitation was recorded in just 18 minutes (Table 2). KCXX legacy precipitation estimates (dual-polarization data not available) over the City and ravine proper were quite impressive, showing accumulations ranging from 6 to 12 mm (0.25 to 0.50 inches) at 5 minutes, 12-25 mm (0.50 to 1.00 inches) at 12 minutes, and 25-37 mm (1 to 1.5 inches) at 29 minutes (Fig. 13). The estimates differ slightly from the observed totals at KBTV given the sites' geographical separation. However, both the observed and estimated short-duration rates were equal to or greater than 25 mm in 30 minutes in this case, supporting the box and whisker analysis that intense rainfall bursts of 25.4 mm (1 inch) or greater in the 30 to 45-minute time step are sufficient in many cases to produce flooding in poor drainage areas of the City.

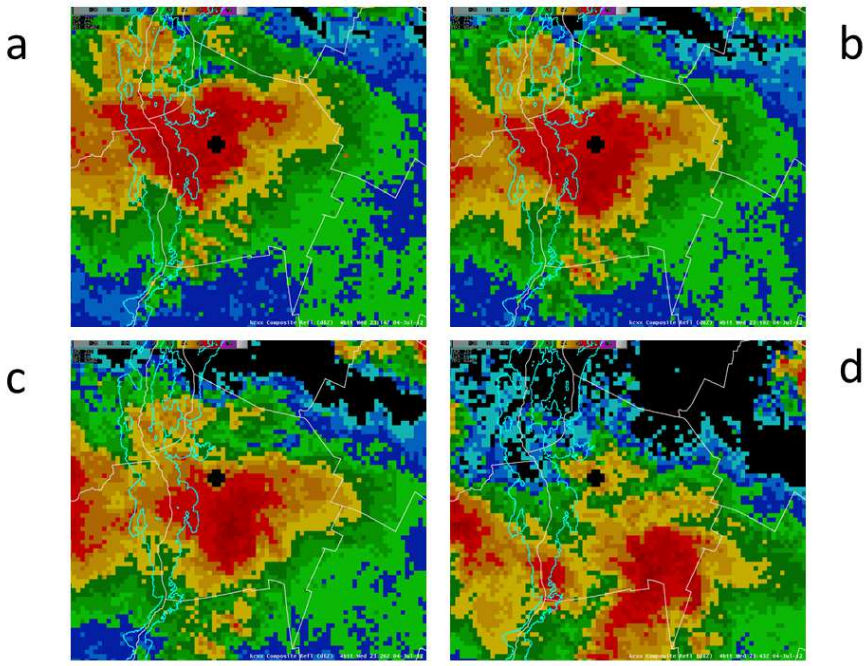

Figure 12 Composite radar reflectivity (dBZ) from the KCXX radar (black cross at the center) obtained during the severe thunderstorm event on 4 July 2012 at 2314 UTC (a), 2319 UTC (b), 2326 UTC (c) and 2343 UTC (d). County boundaries are overlain.

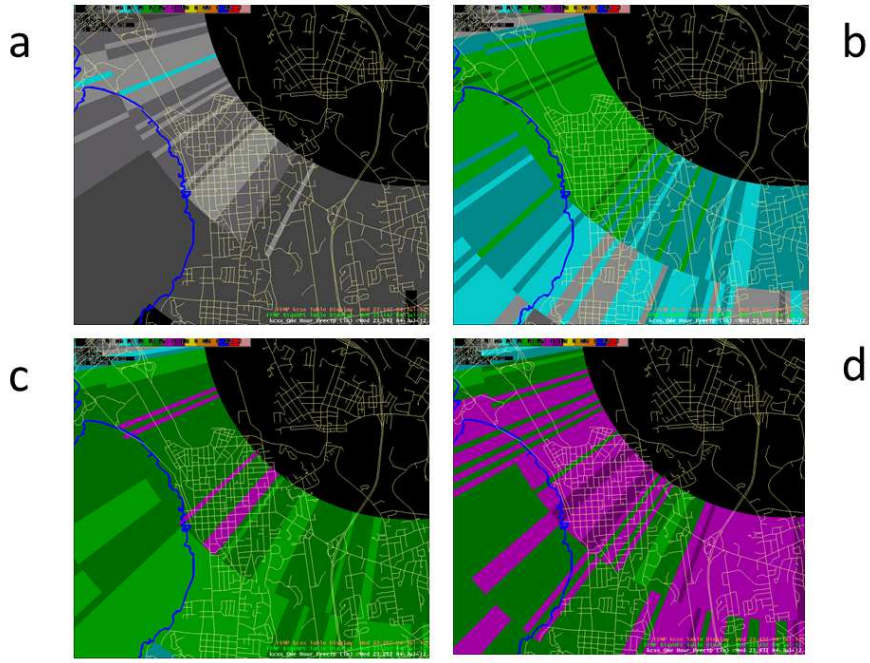

Figure 13 As for Figure 12, but showing 1 hour legacy precipitation estimates of the same event.

Of particular interest was the concentration of flooding reports along the original ravine drainage during this event, which in some cases resulted in tens of thousands of dollars in monetary losses (Thurston 2014). This is illustrated clearly in geospatial plots of observed flooding locations (Fig. 6). Additionally, several of the flooding locations occurred in what appear to be natural depressions along the drainage. As aforementioned, these are clearly shown on both the 1869 Beers Map and the 1872 Coast Survey Map of the City (Fig. 3) and were likely swampy or marshy areas historically, given the lack of infrastructure seen in the immediate vicinity. Further, the 2-foot contour lines clearly show that despite 150 years of urban development, these features still exist as subtle depressions on the urban landscape (Fig. 5). While it can be argued that aged stormwater infrastructure or clogged storm drains played a significant role in the flooding, it appears more likely that the intense, short-duration rainfall rates were the primary culprit, especially when considering the urban context in which the event occurred. During the event, much of the near and subsurface flow would have likely become concentrated along the original ravine drainage, and due to other compounding factors mentioned above would have led to enhanced runoff and pooling.

3.4.2 Case study 2 - 22 May, 2013

Less than one year later, a similar though less severe thunderstorm affected the City on the afternoon of 22 May, 2013. Composite KCXX radar reflectivity showed the storm progressing east across the City from approximately 2130 to 2215 UTC (Fig. 14). While wind gusts were not nearly as strong at KBTV as during the 2012 event, short-duration precipitation rates were nearly equivalent as 25.4 mm (1 inch) of rain was observed in less than an hour, with an impressive 24.4 mm (0.96 inches occurring in just 14 minutes between 2154 and 2208 UTC (Table 3). Similar totals were reported in the City which resulted once again in the rapid onset of high water in several locales, many of which were along the ravine and which had also experienced flooding during the 2012 event (Fig. 6).

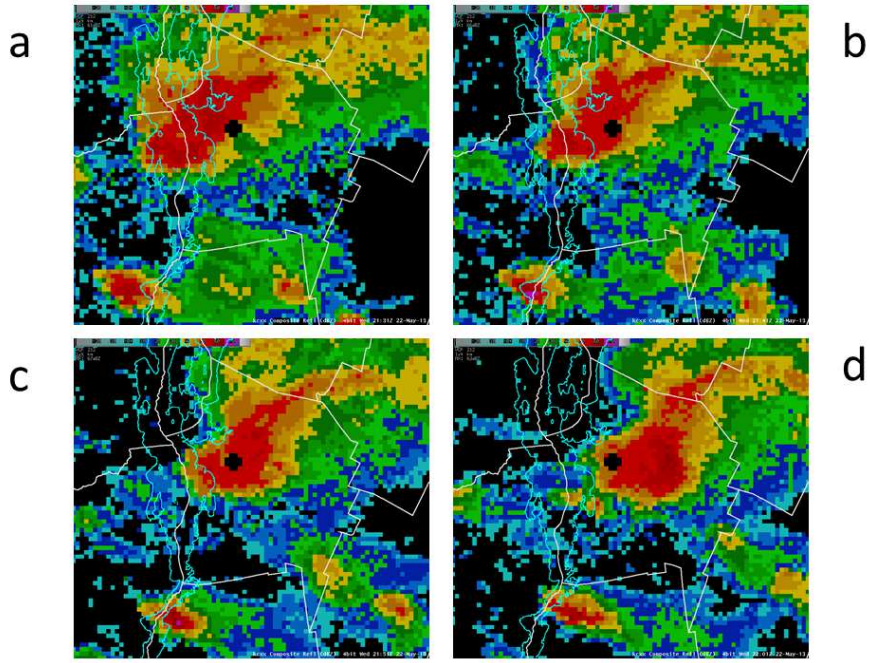

Figure 14 Composite radar reflectivity (dBZ) from the KCXX radar (black cross at the center) obtained during the severe thunderstorm event on 22 May 2013 at 2131 UTC (a), 2141 UTC (b), 2151 UTC (c) and 2201 UTC (d).

From an operational forecasting perspective, added value was gained through interpretation of the dual polarization precipitation products from the KCXX radar, not available during the 2012 event. Unbiased 1-hour DP precipitation estimates showed the increasing intensity of the rainfall during the 30-minute interval between 2131 and 2201 UTC (Fig. 15). Rainfall began around 2130 UTC, then increased dramatically in intensity and rate in the subsequent 30-minute time frame, such that by 2201 UTC areal average DP precipitation estimates in the City were in the 25.4-50.2 mm (1 to 2 inch) range with locally higher totals (Fig. 15 b-d). These amounts more than satisfy the proposed short-duration precipitation rate criterion needed to produce flooding in the City, and in some cases, exceeded those observed in the 2012 event. Further insights from the DP 1-hour precipitation difference estimates (DP minus legacy estimates) (Fig. 16) revealed slightly negative differences at the storm's onset (Figure 16a), which rapidly became positive in subsequent radar scans from 2141 UTC onward. This was likely due to the DP algorithm's capability to identify hydrometeor size, shape and type within the storm, in theory providing better precipitation estimates. By 2201 UTC positive differences as great as 25.4mm (1 inch) were observed in the central portions of the City and along the ravine (Fig. 16d). Perhaps the most valuable DP algorithm during convective rainfall events is that of instantaneous precipitation rate estimates. The 22 May, 2013 event was characterized by varied, sometime intense instantaneous precipitation rates across the City between 2141 and 2156 UTC, in excess of 101.6 mm (4 inches) per hour (orange pixels) during the 15-minute period in many locales and over 152.4 mm (6 inches) per hour (red pixels) in others (Fig. 17). With such intense rainfall rates occurring in such a short period of time, the potential for rapid runoff and resultant urban flooding was increased greatly.

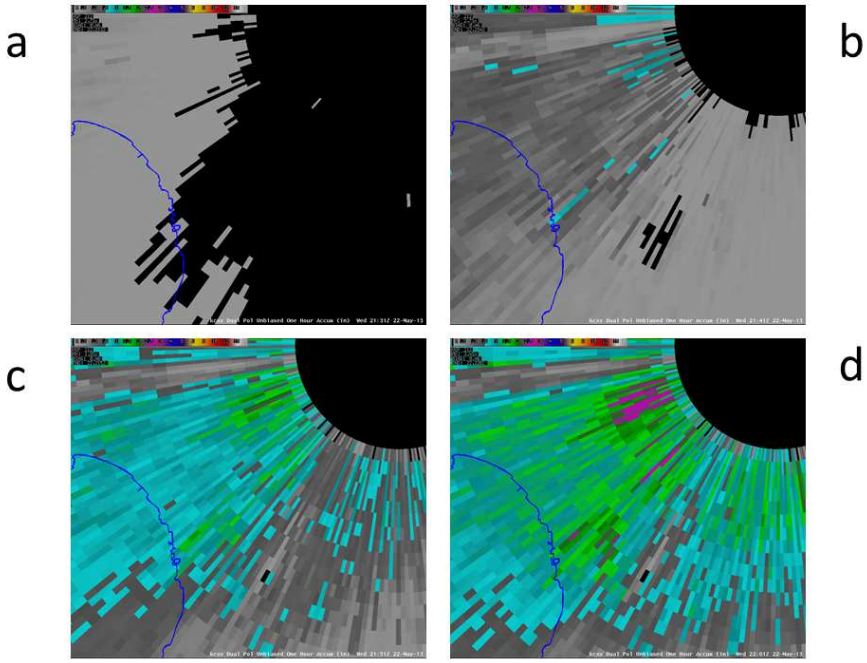

Figure 15 Dual polarized, unbiased 1-hour precipitation estimates (inches/hour) from the KCXX radar for the 22 May 2013 event given on Figure 14 at 2131 UTC (a), 2141 UTC (b), 2151 UTC (c) and 2201 UTC (d). Note the increased spatial resolution obtained from the dual polarization technique.

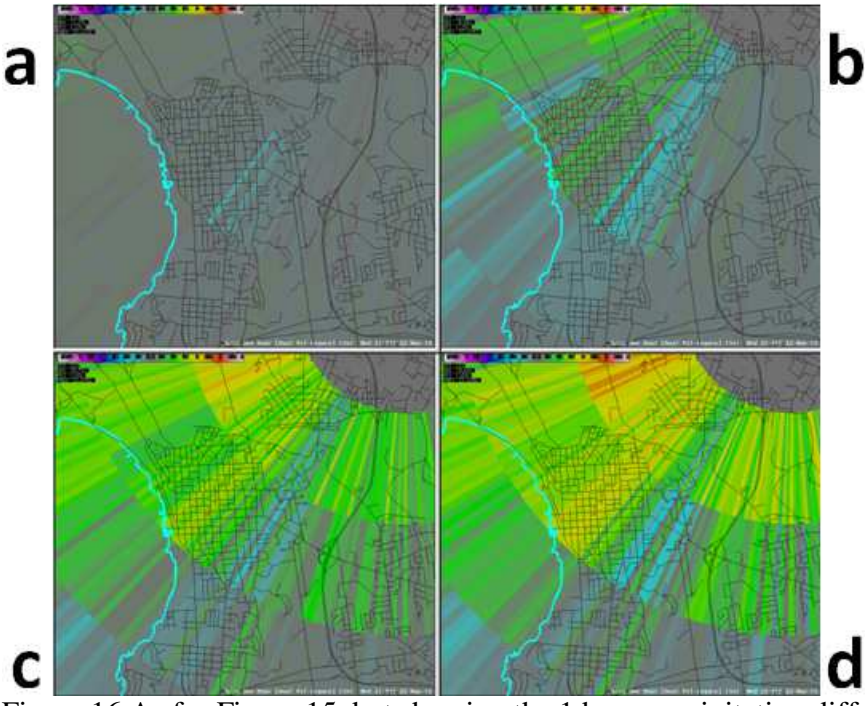

Figure 16 As for Figure 15, but showing the 1 hour precipitation difference estimates (dual polarization - legacy estimates) in inches/hours for the event on 22 May 2013 at 2131 UTC (a), 2141 UTC (b), 2151 UTC (c) and 2201 UTC (d).

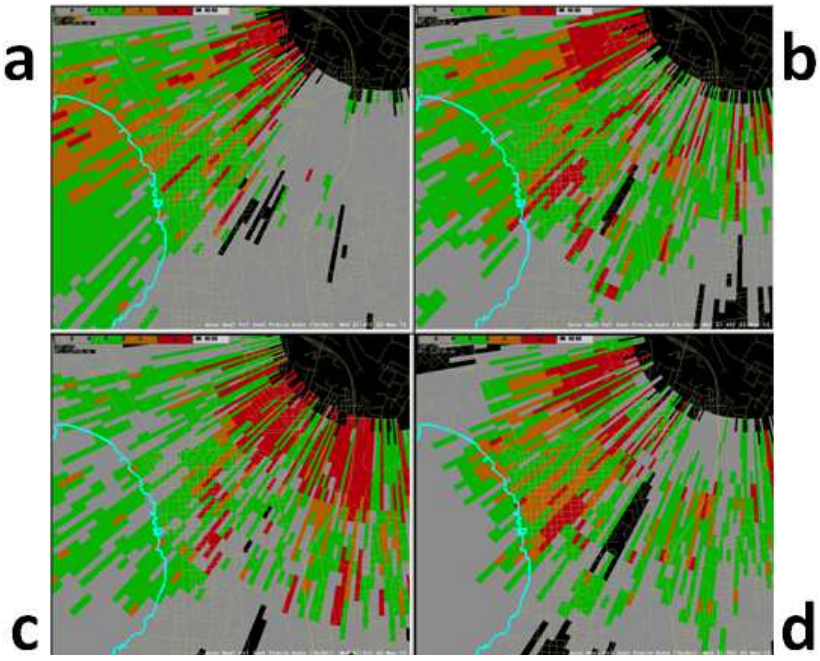

Figure 17 As for Figure 15, but showing the instantaneous precipitation rates (inches/hour) for the event on 22 May 2013 at 2131 UTC (a), 2141 UTC (b), 2151 UTC (c) and 2201 UTC (d).

3.5 Contributing to the Public Works perspective

The foci of repeated flood locations, observed both during the two case studies as well as in archival documents point to the interplay between intense, short duration precipitation and characteristics of the urban morphology. Of particular importance are the location of the aforementioned depressions along the former ravine (Figures 2, 3, 5), the sharp breaks in slope as water flows westward towards the Lake, and the connections between the present-day sewer lines relative to these two factors. For example, 8 of the 9 flooding events observed on 4 July 2012, occurred at the intersection of two sewer lines. Burlington Public Works stormwater managers have speculated that the construction of the modern sewer lines, designed to shunt water away from the ravine sewer system, may actually result in flooding due to a decrease in the overall slope of the system. In addition, two of these flooding locations, observed at the intersection of the sewer lines on Buell and South Union Streets, as well as at Brookes Avenue and US Route 2 and North Willard Street, are marked by an east-west running sewer line in a flatter section of the topography (Figures 1, 5). Three other flood locations were observed at the intersection of Main Street and South Winooski Avenue, where there is a drop in slope near the intersection. This change in slope combined with the intersection of the sewer lines may be a driving factor largely responsible for the flooding. The 9th flooding location on 4 July 2012 occurred in a parking lot on King Street between Church Street and S. Winooski Avenue. The lot lies in a topographic depression and within 65m of a sewer line connection. Two of the three depressions digitized from the 1850s map (Fig. 5) were also clearly identified on the 2-foot (0.3 m) contours (Fig. 6) in the higher elevation portion of the ravine sewer line between Pearl Street and Buell Street (Fig. 6).

4.0 Conclusions and Limitations

This study attempts to gain insight into the historical frequency of flooding in the city of Burlington, VT and identify key meteorological ingredients responsible for such events. Of particular interest is a subtle northeast to southwest oriented ravine which crosses the city and serves as a focal point for flooding and other stormwater-related drainage problems during episodes of intense short-duration rainfall. Historical press articles and NWS Storm Data reveal that flooding is not a new problem to the city with 28 discrete events being cataloged since 1948, approximately 42 percent of all warm season heavy rainfall events that have affected the city during the 65-year study period. While insightful, this methodology did have its limitations as only 2 reliable sources were available. Additionally, it is plausible to assume that not all flooding events were reported, especially if they were of a minor or nuisance category.

Through analysis of precipitation rates it is argued that high intensity rainfall bursts on the sub-hourly time scale have the greatest influence on the urban flood problem in the city. In particular, box and whisker analysis of available short duration precipitation data from 27 flood events show that median rainfall was approximately 1 inch (25 mm) in the 30 and 45-minute time interval. Given that these excessive short term totals fell in a heavily urbanized environment, a portion of which lies within a poorly draining natural ravine, it is not surprising that the City observed flooding during these episodes. On the other hand, plots of 1 and 2 week antecedent precipitation yielded inconclusive results with varying degrees of wet and dry periods observed during both flood and null events. Short-duration precipitation data were limited to 44 of the 67 heavy rainfall events originally identified for this study, with NCDC data only available from 1971 onward. Thus, it could be argued that a more robust dataset is needed to provide conclusive results. The urban flood problem is unique in the sense that stormwater drainage system efficiency and the degree of impervious surfaces can play a significant role in the areal coverage and severity of precipitation runoff. It is known that older portions of Burlington's stormwater drainage system along the ravine have become overwhelmed in a recent series of heavy rainfall events during 2012 and 2013. GIS analysis of known flooding events alongside modern and historic topographic data can allow for a more thorough understanding of the potential influence of topography, in conjunction with known storm water sewer systems inefficiencies, upon flooding events. While this paper does not fully address the combination factors, it points to their consideration in the overall context of the urban flood phenomenon.

Finally, two recent flood events in the city were analyzed using automated surface observations from Burlington International Airport and data from the WSR-88D radar in Colchester, VT (KCXX). Observed and radar-estimated precipitation data show that intense, short-duration precipitation bursts on the order of 1 inch (25 mm) in less than 30 minutes occurred during each episode. The latter case had the added benefit of dual-polarization precipitation algorithms, which gave specific insight into estimated instantaneous precipitation rates at 5 minute intervals. During a 15-minute period radar-estimated rates ranged from 4 to greater than 6 inches per hour across a large portion of the city including the ravine drainage. These observations corroborate findings from the box and whisker short-duration precipitation data that high intensity rainfall bursts of an inch (25 mm) or more on sub-hourly time frames is sufficient to enhance the potential for flooding in the city.

Several contributions to knowledge resulted from the synthesis of hydrometeorological, geospatial, historical and operation engineering analyses. First, the importance of using sub-hourly precipitation totals reinforced anecdotal Department of Public Works observations of the timing most conducive to flooding. Secondly, the analyses presented in this paper address the issue of surface flooding only, and do not capture either the flood events that have occurred in residential basements or within sewer/other pipe dynamics (e.g. as a result of inlet capacity and pipe capacity) that could have also been important critical factors. Finally, data sparsity in the sampling of the precipitation and drainage across the urban catchment, may have contributed to

some of the counter-intuitive results (e.g. the lower importance of antecedent precipitation) that were observed.

Acknowledgements

This research did not receive any specific grant from funding agencies in the public, commercial, or not-for-profit sectors.

References

1. Bedient, P., A. Holder., J. Benavides, and B. Vieux, 2003: Radar-Based Flood Warning System Applied to Tropical Storm Allison. *J. Hydrol. Eng.*, **8**, 308-318.
2. Bedient, P., A. Holder, J. Thompson, and Z. Fang, 2007: Modelling of Storm-Water Response Under Large Tailwater Conditions: Case Study for the Texas Medical Center. *J. Hydrol. Eng.*, **12**, 256-266.
3. Berne, A., G. Delrieu, J.-D. Creutin, and C. Obled, 2004: Temporal and spatial resolution of rainfall measurements required for urban hydrology. *J. Hydrol.*, **299**, 166-179.
4. Blumenfeld, K. A., and R. H. Skaggs, 2011: Using a high-density rain gauge network to estimate extreme rainfall frequencies in Minnesota. *Appl. Geogr.*, **31**, 5-11.
5. Brauer, C. C., A. J. Teuling, A. Overeem, Y. van der Velde, P. Hazenberg, P. M. M. Warmerdam, and R. Uijlenhoet, 2011: Anatomy of extraordinary rainfall and flash flood in a Dutch lowland catchment. *Hydrol. Earth Syst. Sci.*, **15**, 1991-2005.
6. Burlington, VT Public Works cited 2014: Current Stormwater Projects. [Available online at http://www.burlingtonvt.gov/DPW/Stormwater/Projects.]
7. Chintalapudi, S., H. O. Sharif, S. Yeggina, and A. Elhassan, 2012: Physically Based, Hydrologic Model Results Based on Three Precipitation Products. *J. Am. Water Resour. Assoc.*, **48**, 1191-1203.
8. Ciach, G. J., and W. F. Krajewski, 1999: On the estimation of radar rainfall error variance. *Adv. Water Resour.* **22**, 585-595.
9. Collier, C. G., 1986: Accuracy of rainfall estimates by radar, part II: Comparison with raingauge network. *J. Hydrol.*, **83**, 225-235.
10. Creutin, J. D., M. Borga, C. Lutoff, A. Scolobig, I. Ruin, and L. Créton-Cazanave, 2009: Catchment dynamics and social response during flash floods: the potential of radar rainfall monitoring for warning procedures. *Meteorol. Appl.*, **16**, 115-125.
11. Davis, R. S., and P. Jendrowski, 1996: The Operational Areal Mean Basin Estimated Rainfall (AMBER) Module. *Preprints, 15th Conf. on Wea. Analysis and Forecasting,* Norfolk, VA., Amer. Meteor. Soc., 332-335.
12. Davis, R. S. 2003: Some Practical Applications of Flash Flood Monitoring and Prediction, *Preprints, 17th Conference on Hydrology,* Long Beach, CA, CD-ROM, J4.7.
13. Diaz-Nieto, J., D. N. Lerner, A. J. Saul, and J. Blanksby, 2011: GIS Water-Balance Approach to Support Surface Water Flood-Risk Management. *J. Hydrol. Eng.*, **17**, 55-67.
14. Doswell III, C. A., H. E. Brooks and R. A. Maddox, 1996: Flash Flood Forecasting: An Ingredients-Based Methodology. *Wea. Forecasting,* **11**, 560-581.
15. Dupigny-Giroux, L.-A. Hanning, J. R. and Engstrom, E. (2006): Orographic Influence on Frontally-Produced Flooding in Northern Vermont – The 14-15 July 1997 Event, *Phys. Geogr.*, **26**, No. 2, 1-38.
16. Einfalt, T., K. Arnbjerg-Nielsen, C. Golz, N.-E. Jensen, M. Quirmbach, G. Vaes, and B. Vieux, 2004: Towards a roadmap for use of radar rainfall data in urban drainage. *J. Hydrol.*, **299**, 186-202.
17. Huang, Y., Chen, S., Cao, Q., Hong, Y., Wu, B., Huang, M., Qiao, L., Zhang, Z., Li, Z., Li, W. and Yang, X. 2014: Evaluation of Version-7 TRMM Multi-Satellite Precipitation Analysis Product during the Beijing Extreme Heavy Rainfall Event of 21 July 2012. *Water*, **6**, 32-44.
18. Illingworth, A. J., T. M. Blackman, and J. W. F. Goddard, 1999: Improved rainfall estimates in convective storms using polarisation diversity radar. *Hydrol. Earth Syst. Sc.*, **4**, 555-563.
19. Jahanbazi, M., and U. Egger, 2014: Application and comparison of two different dual drainage models to assess urban flooding. *Urban Water J.*, **11**, 584-595.
20. Javier, J., J. Smith, M. Baeck, and G. Villarini, 2009: Flash Flooding in the Philadelphia Metropolitan Region. *J. Hydrol. Eng.*, **15**, 29-38.

21. Jensen, N. E., and L. Pedersen, 2005: Spatial variability of rainfall: Variations within a single radar pixel. *Atmos. Res*., **77**, 269-277.
22. Jessup, S. M., and A. T. DeGaetano, 2007: A Statistical Comparison of the Properties of Flash Flood and Non-flooding Precipitation Events in Portions of New York and Pennsylvania. *Wea. Forecasting*, **23**, 114-130.
23. Jessup, S. M., and S. J. Colucci, 2012: Organization of Flash-Flood-Producing Precipitation in the Northeast United States. *Wea. Forecasting*, **27**, 345-361.
24. Kalin, L., and M. Hantush, 2006: Hydrologic Modeling of an Eastern Pennsylvania Watershed with NEXRAD and Rain Gauge Data. *J. Hydrol. Eng*., **11**, 555-569.
25. Knebl, M. R., Z. L. Yang, K. Hutchison, and D. R. Maidment, 2005: Regional scale flood modeling using NEXRAD rainfall, GIS, and HEC-HMS/RAS: A case study for the San Antonio River Basin Summer 2002 storm event. *J. Environ. Manage*, **75**, 325-336.
26. Krajewski, W. F., A. Kruger, and V. Nespor, 1998: Experimental and numerical studies of small-scale rainfall measurements and variability. *Water Sci. Technol*., **37**, 131-138.
27. Kulkarni, A. T., J. Mohanty, T. I. Eldho, E. P. Rao, and B. K. Mohan, 2014: A web GIS based integrated flood assessment modeling tool for coastal urban watersheds. *Comput. Geosci*., **64**, 7-14.
28. Library of Congress, [Plan of the city of Burlington shewing i.e. showing water & sewer service]. [185-?] [Map] Retrieved from the Library of Congress, Available at <https://www.loc.gov/item/2011589282>. Last accessed 6 June 2016.
29. Maddox, R. A., C. F. Chappell, and L. R. Hoxit, 1979: Synoptic and mesoscale aspects of flash flood events. *Bull. Amer. Meteor. Soc*., **60**, 115-123.
30. Mark, O., C. Wennberg, T. van Kalken, F. Rabbi, and B. Albinsson, 1998: Risk analyses for sewer systems based on numerical modelling and GIS. *Safety Sci.,* **30**, 99-106.
31. Moawad, M. B., 2013: Analysis of the flash flood occurred on 18 January 2010 in wadi El Arish, Egypt (a case study). *Geomat. Nat. Haz. Risk*, **4**, 254-274.
32. Pathirana, A., S. Tsegaye, B. Gersonius, and K. Vairavamoorthy, 2011: A simple 2-D inundation model for incorporating flood damage in urban drainage planning. *Hydrol. Earth Syst. Sc*., **15**, 2747-2761.
33. Peleg, N., M. Ben-Asher, and E. Morin, 2013: Radar subpixel-scale rainfall variability and uncertainty: lessons learned from observations of a dense rain-gauge network. *Hydrol. Earth Syst. Sci*., **17**, 2195-2208.
34. Shahapure, S. S., T. I. Eldho, and E. P. Rao, 2011: Flood Simulation in an Urban Catchment of Navi Mumbai City with Detention Pond and Tidal Effects Using FEM, GIS, and Remote Sensing. *J. Waterw. Port. C. Asce.*, **137**, 286-299.
35. Shih, D.-S., C.-H. Chen, and G.-T. Yeh, 2014: Improving our understanding of flood forecasting using earlier hydro-meteorological intelligence. *J. Hydrol*., **512**, 470-481.
36. Smith, S. B., M. Churma, J. Roe, and L. Xin, 2000: Flash Flood Monitoring and Prediction in AWIPS Build 5 and Beyond. *Preprints, 15th Conf. on Hydrology,* Long Beach, CA, Amer. Meteor. Soc., 229-232.
37. Smith, J. A., M. L. Baeck, K. L. Meierdiercks, A. J. Miller, and W. F. Krajewski, 2007: Radar rainfall estimation for flash flood forecasting in small urban watersheds. *Adv. Water Resour*., **30**, 2087-2097.
38. Smith, J. A., M. L. Baeck, G. Villarini, D. B. Wright, and W. Krajewski, 2013: Extreme Flood Response: The June 2008 Flooding in Iowa. *J. Hydrometeor*., **14**, 1810-1825.
39. Tehrany, M. S., B. Pradhan, and M. N. Jebur, 2014: Flood susceptibility mapping using a novel ensemble weights-of-evidence and support vector machine models in GIS. *J. Hydrol*., **512**, 332-343.
40. Thurston, Jack. "Flash Flood Forces Closure of Vt. Homeless Center." New England Cable

News. Published March 21, 2014. Accessed October 9, 2014. [Available online at: www.necn.com/news/new-england/_NECN_Flash_Flood_Forces_Closure_of_VT_Homeless_Center_NECN-251620401.html.]
41. Vasiloff, S., 2012: Evaluation of Dual-Polarization QPE: Initial Results for Spring and Summer 2012. WSR-88D Radar Operations Center Final Report, Memorandum of Understanding Task 1.1, 48pp, [Available online at: http://www.roc.noaa.gov/wsr88d/PublicDocs/AppsDocs/Eval_DualPol_QPE_Initial_results_spring_summer_2012.pdf].
42. Viavattene, C., and J. B. Ellis, 2013: The management of urban surface water flood risks: SUDS performance in flood reduction from extreme events. *Water Sci. Technol.*, **67**, 99-108.
43. Vieux, B. E., and J. E. Vieux, 2005: Statistical evaluation of a radar rainfall system for sewer system management. *Atmos. Res.*, **77**, 322-336.
44. Yoo, C., J. Yoon, and E. Ha, 2013: Detection of mean-field bias of the radar rain rate using rain gauges available within a small portion of radar umbrella: a case study of the Donghae (East Sea) radar in Korea. *Stoch. Env. Res. Risk A.*, **27**, 423-433.

Table 1 KBTV METAR observations during the severe thunderstorm event on 04 July, 2012 showing strong wind gusts in excess of25 ms-1 (50 kt).

TIME (UTC)	KBTV METAR OBSERVATIONS
2321	SPECI KBTV 042321Z 33028G51KT 1/8SM +TSRA FG SCT016 BKN050 OVC100 22/20 A2968 RMK AO2 PK WND 32051/2321 RAB2258 FRQ LTGCCCG OHD P0006 RVRNO
2325	SPECI KBTV 042325Z 32037G55KT 1/8SM +TSRA FG SQ SCT009 BKN024 OVC100 21/19 A2973
2329	SPECI KBTV 042329Z 33013G55KT 300V360 1/8SM +TSRA FG SQ BKN009 BKN055 OVC080 20/19 A2974 RMK AO2 PK WND 32055/2322 WSHFT 2315 RAB2258 PRESRR FRQ LTGCCCG OHD P0044 RVRNO
2332	SPECI KBTV 042332Z 35011G52KT 1/2SM +TSRA FG BKN011 BKN055 OVC090 20/19 A2974 RMK AO2 PK WND 32055/2322 WSHFT 2315 RAB2258 FRQ LTGCCCG OHD P0065 RVRNO

Table 2 Heavy short-duration precipitation totals at KBTV associated with the severe thunderstorm event on 04 July, 2012.

TIME (UTC)	PRECIPITATION TOTAL (mm)
2318	1.016
2321	1.524
2325	N/A
2329	11.176
2332	16.51
2339	25.4
2354	27.178

Table 3 Heavy short-duration precipitation totals at KBTV associated with the thunderstorm event on 22 May, 2013.

TIME (UTC)	PRECIPITATION TOTAL (mm)
2152	1.27
2154	2.286
2156	4.318

2208	26.67
2215	27.432
2226	28.194
2242	28.956